Version of Record: https://www.sciencedirect.com/science/article/pii/S1540748918305583
Manuscript_3ad6a20d41d7364d8aa675d6a0b67127

# Kinetic modeling study of surrogate components for gasoline, jet and diesel fuels: C7-C11 methylated aromatics

Goutham Kukkadapu*[a], Dongil Kang[b], Scott. W. Wagnon[a], Kuiwen Zhang[a], Marco Mehl[a], M. Monge-Palacios[c], Heng Wang[c], S. Scott Goldsborough[b], Charles K. Westbrook[a], William. J. Pitz[a]

[a] Lawrence Livermore National Laboratory, Livermore, CA 94551.

[b] Argonne National Laboratory, Argonne, IL 60439.

[c] King Abdullah University of Science and Technology, Thuwal, Saudi Arabia 23955.

Corresponding Author:

Goutham Kukkadapu

Lawrence Livermore National Laboratory

7000 East Avenue

Livermore, CA 94551, USA

E-Mail: kukkadapu1@llnl.gov

Phone: (925) 422-1489

**Colloquium: Gas Phase Reaction Kinetics**

**Total length of paper= 3537+1904+734+76=6198 words (Method 1)**

**Word count from main text= 3479**

**Total word count from figures= 1848**

| | Height in mm | # of columns | # of words in caption | Word count |
|---|---|---|---|---|
| Figure 1 | 71.12 | 2 | 26 | 383 |
| Figure 2 | 55.86 | 1 | 30 | 173 |
| Figure 3 | 39.37 | 1 | 30 | 135 |
| Figure 4 | 74.93 | 2 | 32 | 400 |
| Figure 5 | 38.64 | 1 | 23 | 130 |
| Figure 6 | 39.37 | 2 | 31 | 248 |
| Figure 7 | 39.37 | 2 | 20 | 237 |
| Figure 8 | 43.18 | 1 | 28 | 145 |

**Total word count from Tables= (8 text line + 2 blank) X 7.6** (7.6 words/line) =76 words

**Total word count from References**= (40+2) x (2.3 lines/reference) X (7.6 words/line) = **734 words.**

**Affirmation to pay color reproduction charges if applicable:** Yes

**Supplementary material available**

## Abstract

Kinetic mechanisms for aromatics are needed to successfully simulate the autoignition of transportation fuels using the surrogate fuel approach. An aromatic detailed kinetic mechanism that describes kinetics of C7-C11 methylated aromatics, including toluene, *o*-xylene, *p*-xylene, 1,2,4-trimethylbenzene, 1,3,5, trimethylbenzene and α–methylnaphthalene has been developed in the current study. The kinetic mechanism was built hierarchically using similar set of reaction pathways and reaction rate rules. In the mechanism developed, special emphasis is put on describing the detailed low-temperature ignition chemistry of *o*-xylene and 1,2,4-trimethylbenzene and, to our knowledge, this is the first attempt to do so in a detailed kinetic mechanism. In addition to kinetic modeling, new experimental data were acquired for toluene, *o*-xylene, and 1,2,4-trimethylbenzene using a rapid compression machine at low-to-intermediate temperatures and engine relevant pressures. In addition, the mechanism has been compared against data sets from the literature covering ignition delay times, flame speeds, and speciation profiles measured in a jet-stirred reactor and flow reactor. Good agreement is observed between the mechanism predictions and the experimental data. Kinetic analysis demonstrated the importance of including the low temperature chemistry of the benzylperoxy radicals to accurately capture the ignition propensity of *o*-xylene and 1,2,4-trimethylbenzene at low-to-intermediate temperatures and high pressures. The kinetic mechanism developed in the current study can be used for surrogate modeling of gasoline, jet and diesel fuels.



**Keywords:** Aromatics, Toluene, Xylenes, Trimethylbenzenes, Surrogates.

## 1. Introduction:

Aromatics, one of the important hydrocarbon classes found in transportation fuels [1,2], are known to play a key role in determining combustion properties (eg: octane sensitivity, sooting propensity) and hence are widely used in surrogate fuels. The aromatic fuels found in gasolines are generally monoaromatics while diaromatics are also observed in jet and diesel fuels [1,2]. A deeper understanding of the chemistry and predictive kinetic mechanisms for *mono*- and *di*- aromatics are highly sought to advance in surrogate modeling of gasoline, jet and diesels fuels. Therefore, a detailed kinetic mechanism that describes the oxidation chemistry of toluene, *o*-xylene, *p*-xylene, 1,2,4-trimethylbenzene, 1,3,5-trimethyl benzene and α–methylnaphthalene was developed. Toluene, the xylene isomers, and the trimethylbenzene isomers have been studied as they are of interest to gasoline fuels, while α–methylnaphthalene is commonly used in various jet and diesel surrogate formulations. Furthermore, Roubaud *et al.* [3] reported that the isomers of xylene and trimethylbenzene exhibit significant differences in ignition propensities and the reason for the observed differences was attributed to the possible low-to-intermediate temperature chemistry between the *ortho*- substituted methyl groups. Hence, in the kinetic mechanism developed here, particular emphasis was placed on describing the low-to-intermediate temperature chemistry of *o*-xylene, and 1,2,4-trimethylbenzene to capture the effect of substitution interactions on ignition propensity. As it is known that *m*-xylene and *p*-xylene exhibit similar reactivity, we do not differentiate between *m*- and *p*- xylene in the current mechanism and so, the mechanism of *p*-xylene developed here in can be used to simulate ignition of *m*-xylene too. Finally, the oxidation of toluene, *o*-xylene, *p*-xylene, 1,2,4-trimethylbenzene, 1,3,5-trimethyl benzene and α–methylnaphthalene has been studied using shock tubes [4-7], flow reactors [8-10] and jet stirred reactors [11-15], but there is a dearth of ignition delay data of these aromatics at low-to-intermediate temperatures and engine relevant pressures. Therefore, in this study new experiments were conducted using a rapid compression machine (RCM) with selected aromatics to provide ignition delay times at

low-to-intermediate temperatures and engine relevant pressures which shall serve as valuable validation targets for kinetic modeling. The following sections describe development of the kinetic mechanism, experimental specifications and validation of the kinetic mechanism.

## 2. Development of the kinetic mechanism:

The kinetic mechanism developed in this work is based on the earlier mechanism of Mehl *et al.* [16] and Zhang *et al.* [17] and updates have been conducted to adopt new reaction rates and reaction channels from recent *ab initio* works available in the literature. The base chemistry of AramcoMech 2.0 [18] is used to describe the C0-C4 chemistry. Some important revisions to the mechanism shall be discussed in this section.

### 2.1 Abstraction reactions:

The abstraction reactions from the methyl site by oxygen molecules producing benzylic and hydroperoxyl radical were taken from the study of Oehlschlaeger *et al.* [19]. The rates for H-abstraction reactions by OH and $HO_2$ radicals have been adopted from the studies of Seta *et al.* [20] and Altarawneh *et al.* [21] respectively. The abstraction reactions by H radicals were taken from the work of Baldwin *et al.* [22], while the abstraction by O radicals were taken from the study of Li et al. [23]. During the development of the mechanism it was assumed that the rates of abstractions reactions are unaffected by the steric interaction between the methyl groups based on the findings of Elwardany *et al.* [24]. In their study [24] the differences in rates of H-abstraction by OH radicals from *o*-, *m*- and *p*-xylenes were small (20-30%) and close to the experimental uncertainty (19-24%).

### 2.2 Oxidation of the methyl site:

Kinetics of methylated aromatics is primarily driven by oxidation at the methyl site at low-to-intermediate temperatures and it is imperative to accurately represent the kinetics of oxidation of this site correctly when developing aromatic mechanisms. In the current mechanism, the rate constants and

treatment of the benzylic+O, benzylic+$HO_2$ and benzylic+$O_2$ systems have been updated and shall be described briefly.

The benzylic+O system, an important reaction system at high temperatures, has been adopted from the recent study of da Silva and Bozzelli [25]. In [25] the G3SX composite theoretical method was used and it was found that the benzyl+O reaction system to be dominated by addition reactions at the methylene site producing an excited benzoxyl adduct which subsequently decomposes to produce formyl radical+benzene, and benzaldehyde+H.

The benzyl+$HO_2$ system was studied by da Silva and Bozzelli [26] at G3B3 level of theory. In [26], they found that the formation of the stable benzylhydroperoxide and benzoxyl along with OH are the two important reaction channels in the benzyl+$HO_2$ system. The branching ratios for these reactions exhibited a complex temperature dependence with formation of stable benzylhydroperoxide favored at temperatures below 800 K, while the formation of OH along with benzoxyl radicals is dominant above 800 K. The benzylhydroperoxide subsequently undergoes decomposition reactions predominantly on producing OH along with benzoxyl radicals. The rates of decomposition of benzylhydroperoxide and benzoxyl radicals were adopted from da Silva and Bozzelli [27,28].

Murakami *et al.* [29,30] studied the kinetics of benzyl+$O_2$ and xylyl isomers+$O_2$ systems. In their study [30], they observed the well depth of the association reaction producing the benzylperoxy and oxylylperoxy adducts to be around 21 kcal/mole. This well depth is much lower than the well depths normally observed in analogous reactions of alkyl radicals and hence is very unstable, and quickly decomposes back to benzyl and $O_2$ at low temperatures. However, at high temperatures, the peroxy adduct can undergo unimolecular isomerizations reactions producing benzaldehyde along with OH, and phenoxy and formaldehyde. Murakami *et al.* [30] also noted that the thermochemistry and the reaction channels of the *m*-xylylperoxy and *p*-xylylperoxy radicals were similar to that of benzylperoxy but *o*-xylylperoxy radicals could undergo an isomerization reaction involving the peroxy and the methyl

moieties through a 7-member transition state producing *o*-xylyl hydroperoxy radicals. The reaction rate for this isomerization was adopted from Canneaux *et al.* [31]. The *o*-xylyl hydroperoxyl radicals subsequently can be consumed by addition of $O_2$ or undergo cyclization reaction producing phthalan along with OH. The formation of phthalan+OH was proposed to be reason for the relative higher reactivity of the ortho-substituted aromatics. In the current mechanism, the formation of phthalan and the $O_2$ addition to *o*-xylyl hydroperoxyl radicals have been modelled. The rate of the association reaction producing *o*-peroxy xylyl hydroperoxide has been adopted from the rate of benzyl+$O_2$ reaction [29]. The *o*-peroxy xylyl hydroperoxide can undergo an isomerization reaction producing formyl substituted benzylhydroperoxide which is analogous to the ketohydroperoxides observed in alkane chemistry. As the rate for this reaction is not available in literature, the rate of the analogous reaction from Canneaux *et al.* [31] was used. The formyl substituted benzylhydroperoxide subsequently decomposes to produce phthalaldehyde along with OH and H radicals. The low temperature reactivity of *o*-xylyl+$O_2$ system and its subsequent reactions as noted by da Silva and Bozzelli [32] can be described as the overall reaction *o*-xylyl+$2O_2$ = phthalaldehyde+2OH+H which is highly chain branching, and thus is expected to be the reason for the low temperature reactivity of *o*-xylene. The isomerization reaction of the peroxy radical involving the *ortho*-methyl groups have been modelled to capture the low temperature chemistry of *o*-xylene and 1,2,4-trimethylbenzene.

Another important reaction involving benzylic radicals is self-recombination. The chain terminating self-recombination reaction pathway competes with reactions of benzylic radicals with $HO_2$ and $O_2$ at low temperatures. The rate for the recombination reaction used in toluene and *o*-xylene in the current mechanism are from the study of Matsugi and Miyoshi [33]. In study of [33], the authors noticed that the rate of recombination of *o*-xylyl radicals to be lower than that of benzyl radicals, and the difference in rates was attributed to steric hinderance caused by increased branching. Unfortunately, similar studies on recombination of benzylic radicals produced from H-abstraction from

trimethylbenzene and α–methylnaphthalene are unavailable. Hence, in the current study the rate of recombination reaction of xylyl radicals was used in sub-mechanisms of trimethylbenzenes and α–methylnaphthalene with the A factors reduced to account for the steric hinderances which could increase with size of the molecule. The A factors were reduced by factors of 1.35 and 1.85 in trimethylbenzenes and α–methylnaphthalene sub-mechanisms respectively.

### 2.3 Reactions of phenylic radicals:

The H-abstractions from the aromatic ring produce very reactive phenylic radicals which are primarily consumed by addition reactions with oxygen molecules. The current mechanism describes in detail the reaction channels proposed by da Silva *et al.* [34] which include formation of peroxy adducts, phenoxy radicals and dioxo-hexadienyl radicals.

## 3. Experimental specifications:

Argonne's twin opposed-piston RCM is used for this study. Its capabilities are detailed elsewhere [35], however a brief description is provided here. The reaction chamber has a 50.8 mm bore with a clearance height at maximum compression of 25.5 mm. Creviced pistons are employed to minimize fluid dynamic effects during compression and improve post-compression charge homogeneity. Hydraulic pistons are used to actuate compression and lock the pistons at top dead center (TDC). Compression times are typically less than 16 ms. For this work, the geometric compression ratio (CR) is maintained at 11.5:1. Pressure histories were measured using a thermal shock resistant Kistler 6045A-U20 transducer mounted flush in the side wall of the reaction chamber. The transducer output is conditioned by a Kistler Type 5064 charge amplifier (Model 2852A12) with the signal split and data captured with two cards (NI 9239 (24-bit/50kHz); NI 9223 (16-bit/1000kHz)). In the current study, high purity (99.99%) nitrogen, argon, and oxygen are used which were supplied by Airgas®. The liquid fuels toluene (99.8%), *o*-xylene (99.8%), 1,2,4-trimethylbenzene (98%) from Sigma–Aldrich® were used. The experiments were

conducted at nominal pressures of 25 bar and 45 bar, and equivalence ratios of ϕ=0.5 and 1 in $O_2/N_2$/Ar mixtures containing 12.4% $O_2$. Experiments were not conducted with the fuel-rich mixtures in the present test series due to the weak evaporation characteristics of 1,2,4-trimethylbenzene (124TMB). For the test mixtures shown in Table 1, the experimental facility was heated from 40 to 100 °C, and the ratio of $N_2$ to Ar was varied to cover a range of compressed temperatures. Representative estimates of uncertainty, and statistical variation in facility measurements for the reported IDT's and compressed temperatures are about ± 10% and 0.7%, respectively.

Table 1: Molar composition of the test mixtures.

| | **Toluene** | ***o*-Xylene** | **124TMB** | **$O_2$** | **$N_2$** | **Ar** |
|---|---|---|---|---|---|---|
| ϕ=1 | 1.37 | 0.00 | 0.00 | 12.30 | 25.83 | 60.50 |
| ϕ=0.5 | 0.69 | 0.00 | 0.00 | 12.40 | 34.71 | 52.21 |
| ϕ=1 | 0.00 | 1.17 | 0.00 | 12.32 | 52.00 | 34.50 |
| ϕ=0.5 | 0.00 | 0.60 | 0.00 | 12.41 | 60.97 | 26.02 |
| ϕ=1 | 0.00 | 0.00 | 1.03 | 12.33 | 51.99 | 34.66 |
| ϕ=0.5 | 0.00 | 0.00 | 0.52 | 12.42 | 60.99 | 26.07 |

## 4. Results:

The performance of the current kinetic mechanism in estimating the ignition delay time (IDT) measured in the Argonne RCM shall be shown first, followed by validations against literature data.

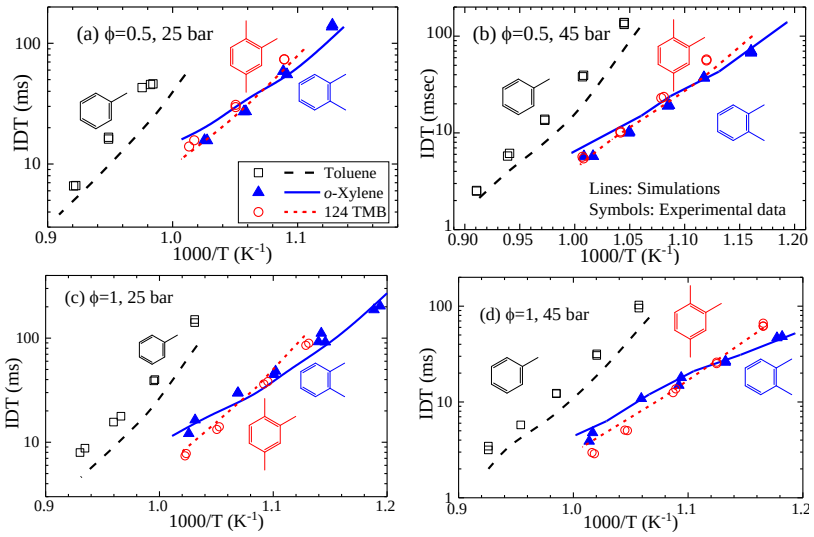

Figure 1: Comparison of experimental and simulated IDT's of toluene, *o*-xylene and 1,2,4-trimethylbenzene (124TMB) at varying temperature, pressure and equivalence ratios measured in the current study.

### 4.1 Validation against data from current study

Figure 1 shows the comparison of experimental and simulated IDT's of toluene, *o*-xylene and 1,2,4-trimethylbenzene (124TMB) at different test conditions investigated in the current study. Unlike in previous work [36,37] there was little evidence of non-uniform ignition phenomena across all of the test conditions explored here, as demonstrated in the Fig. S1. As expected, toluene was found to be least reactive at test conditions below about 1000 K. This lower reactivity of toluene compared to *o*-xylene and 1,2,4-trimethylbenzene is well predicted by the kinetic mechanism. An interesting trend was observed in the comparison of the experimental reactivity of *o*-xylene and 1,2,4-trimethylbenzene. The experimental IDT's suggest that *o*-xylene is more reactive than 1,2,4-trimethylbenzene at low temperatures while 1,2,4-trimethylbenzene becomes more reactive than *o*-xylene at high temperatures. The cross over in reactivity observed around 900 K is also captured by the kinetic mechanism developed herein which is very encouraging given the that the current mechanism is the one of the first attempts, to our knowledge, to simulate the low temperature reactivity of *o*-xylene and 1,2,4-trimethylbenzene. Besides capturing the relative reactivity of *o*-xylene and 1,2,4-trimethylbenzene, the mechanism also appears to do a good-to-excellent job in predicting the ignition delay with the differences in experimental and simulated IDT's generally within 20% of the experimental values. However, the experimental and simulated IDT's of toluene show slightly higher differences, with the simulated IDT's of toluene consistently shorter than the experimental counterparts by about 30-35% for the test conditions investigated in this study.

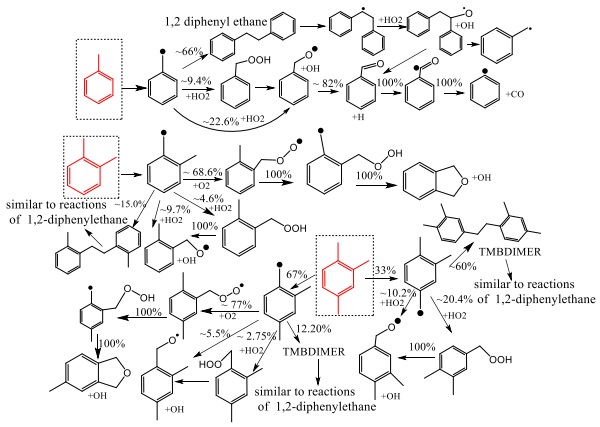


Figure 2: Plot showing the important reaction channels of toluene, *o*-xylene and 1,2,4-trimethylbenzene at ~ 20% fuel conversion. Initial temperature=900 K, initial pressure = 45 atm, ϕ=1 mixtures from Table 1.

As the mechanism was able to predict the reactivity trends and the IDT's reasonably well, reaction path analysis was conducted to gain insights into the ignition chemistry of toluene, *o*-xylene and 1,2,4-trimethylbenzene. From the reaction path analysis (shown in Fig. 2), it can be seen that the chemistry of toluene, *o*-xylene and 1,2,4-trimethylbenzene is dominated by the abstractions from the methyl sites, and the reactivity of the system is controlled by the fate of the benzylic radicals for the conditions investigated. In the case of toluene, the consumption of benzyl radicals was found to be dominated by chain termination reactions (~66%) producing 1,2-diphenylethane while in the case of *o*-xylene, the *o*-xylyl radicals are consumed primarily (~56%) by reactions with $O_2$ producing o-xylylperoxy radicals which undergo internal isomerization reactions and subsequently produce phthalan and OH radical, and facilitate chain propagation reactions. Finally, in the case of 1,2,4-trimethylbenzene, the H abstractions from methyl groups at 1 and 2 (*ortho*- sites) produce benzylic radicals which behave similarly to *o*-xylyl radicals facilitating chain propagation reactions(in the current mechanism, these two isomeric radicals are lumped, and hence only one radical is shown in the figure).

The radical produced by H-abstraction reaction from the methyl group on 4 site (*para*-) in 1,2,4-trimethylbenzene however behaves like benzyl radical facilitating chain termination reactions.

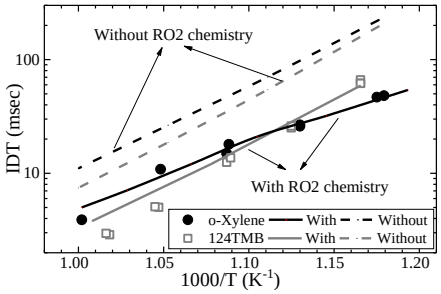


Figure 3: Plot showing the effect of "turning off" the $RO_2$ internal isomerization pathways on ignition propensity of $\phi$=1, 12.4% $O_2$ fuel/$O_2$/$N_2$/Ar mixtures of *o*-xylene and 1,2,4-trimethylbenzene at 45 bar.

As the reaction path analysis shows high amount of flux through the addition of $O_2$ to the benzylic sites in *o*-xylene and 1,2,4-trimethylbenzene, simulations were conducted to assess the importance of these low temperature paths for autoignition. In this analysis, the internal isomerization reactions of the benzylperoxy adducts ($RO_2$) of *o*-xylene and 1,2,4-trimethylbenzene were turned off in the chemical kinetic mechanism and the results compared to the mechanism with these reactions included (Fig. 3). As seen in Fig. 3, isomerization reactions are important not only to the capture the reactivity of the *o*-xylene and 1,2,4-trimethylbenzene, but also to capture the relative reactivities. This analysis also helps briefly explain, as follows, the crossover in reactivity of *o*-xylene and 1,2,4-trimethylbenzene. Based on degeneracy, only 67% (from abstraction of H from methyl at sites 1, 2) of the benzylic radicals produced from 1,2,4-trimethylbenzene could facilitate chain propagation (or chain branching) pathways at low temperatures while in the case of *o*-xylene, all (100%) of the *o*-xylyl radicals can facilitate chain propagation pathways (or chain branching), so the enhancement of ignition propensity from the low temperature $RO_2$ chemistry would be higher in the case of *o*-xylene than compared to 1,2,4-trimethylbenzene. From Fig. 3, the mechanism suggests that in the absence of low temperature $RO_2$ chemistry the difference in reactivity of *o*-xylene and 1,2,4-trimethylbenzene is

marginal at low temperatures (T<870 K). Hence, the higher enhancement in ignition propensity from the $RO_2$ chemistry would make *o*-xylene more reactive than 1,2,4-trimethylbenzene at low temperatures. However, at high temperatures the enhancing effect of the $RO_2$ chemistry diminishes due to the lower stability of the peroxy adduct making 1,2,4-trimethylbenzene become more reactive than *o*-xylene resulting in a crossover in reactivity.

### 4.2 Validations against literature data:

In the current section, the validations of the mechanism against the ignition delay data and the speciation data available in the literature are shown. Furthermore, it is noted that the current kinetic mechanism is built hierarchically using similar set of reaction pathways and reaction rates, and hence, can be used to simulate the ignition of *p*-xylene, 1,3,5-trimethylbenzene and α-methylnaphthalene, as well. To demonstrate the ability of the mechanism to capture the ignition of *p*-xylene and 1,3,5-trimethylbenzene and α-methylnaphthalene, the validation targets were chosen to include the ignition data of these three aromatics along with additional data of toluene, *o*-xylene and 1,2,4-trimethylbenzene.

#### 4.2.1 Ignition delay validations

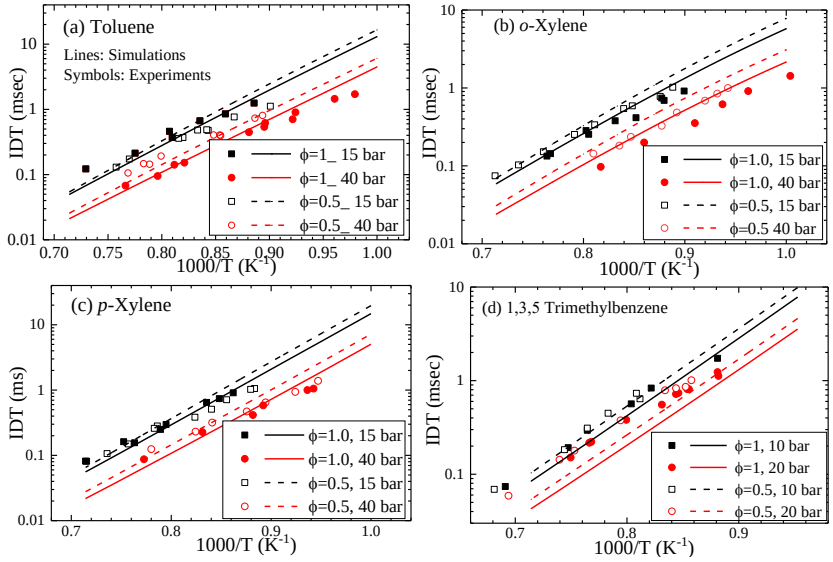

Figure 4: Comparisons of IDT's of monoaromatics (a) toluene [4], (b) *o*-xylene [5], (c) *p*-xylene [5], (d) 1,3,5-trimethylbenzene [6] in air. Constant volume adiabatic simulations were conducted to compare against ST data.

Figures 4 and 5 show simulated and literature IDT's of methyl substituted mono- and di-aromatics. As seen from Fig. 4, the mechanism does an acceptable job in general in predicting the IDT's of the toluene, *p*-xylene and 1,3,5-trimethylbenzene at varying pressure, temperature and equivalence ratios. However, differences are clearly observed in the comparisons of IDT's of *o*-xylene and α-methylnaphthalene. In Fig. 5, the mechanism is found to perform excellently against the ignition delay data of α-methylnaphthalene at fuel lean conditions of ϕ=0.5, but the mechanism under predicts the reactivity at low temperature stochiometric conditions, ϕ=1. Reasons for the observed discrepancy in dependence on equivalence ratio are not clear. Possible explanations include the effect on an additional aromatic ring on the kinetics of the benzylic+$HO_2$ system in α–methylnaphthalene and because of yet still unresolved chemistry in the α-methylnaphthalene.

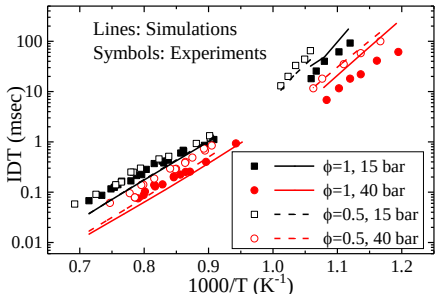


Figure 5: Plot showing comparisons of IDT's of α-methylnaphthalene/air mixtures [7,38]. 0-D simulations with volume histories were conducted for comparing the RCM IDT's.

### 4.2.2 Flow reactor validations

Oxidation of alkyl aromatics has been extensively studied in the Princeton flow reactors by Glassman, Brezinsky, Dryer, and co-workers [6,8-10]. Figure 6 shows validations against the oxidation

of near stochiometric (ϕ=0.977), 0.14 % toluene/$O_2$/$N_2$ mixtures conducted at elevated pressure of 12.5 atm and an initial temperature of 920 K from [8]. As seen from Fig. 6a, the mechanism successfully predicts the conversion profiles of $O_2$ and fuel, and also the evolution of the major intermediates which include carbon oxides, water, benzene, formaldehyde. In Fig 6b, significant differences are observed in concentrations of methane, but the concertation of the methane in JSR (c.f., Fig. S5) of toluene at similar pressure and temperature conditions is very well captured by the model and reason for the difference observed in fig. 6b is not clear. At these conditions, the oxidation of toluene was found to be controlled by the competition between the chain terminating recombination reaction of benzyl radicals producing 1,2-diphenylethane and the chain branching reactions initiated by reaction of benzyl+ $HO_2$ which can be summarized by an overall reaction of benzyl+HO2=> benzaldehyde+OH+H.

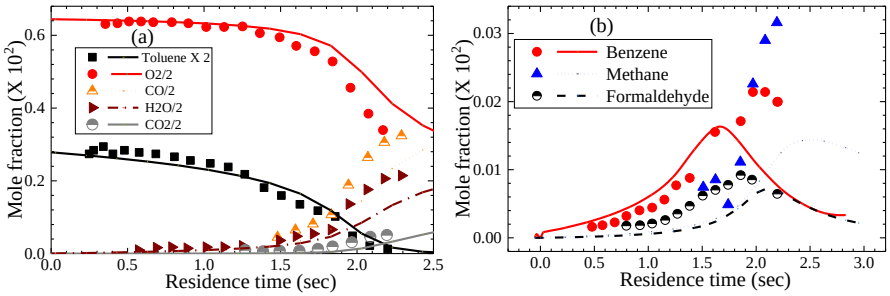


Figure 6: Comparison of major intermediates produced during oxidation of ϕ=0.977 0.14 % toluene/$O_2$/$N_2$ mixtures [8] at pressure of 12.5 atm in a flow reactor. Experimental data shifted by +0.25 s.

### 4.2.3 JSR validations

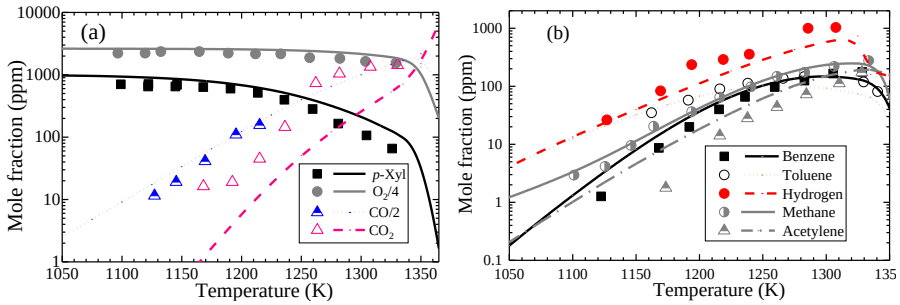


Figure 7: Comparison of major intermediates produced during JSR oxidation of stochiometric 0.10 % p-Xylene/$O_2$/$N_2$ mixtures [12] at atmospheric pressure, residence time=0.1s.

Oxidation of the aromatics in a jet stirred reactor at similar test conditions was studied extensively by Dagaut and co-workers [11-13]. From their different studies, we have taken oxidation data of stochiometric *p*-xylene ($X_{fuel}$=0.1 %)/O2/N2 mixtures [12] for the current validations and the comparisons of the speciation profiles of fuel, toluene, benzene, acetylene, methane, $O_2$, carbon oxides, hydrogen are shown in Fig. 7. As seen in Figs. 7a and 7b the mechanism successfully captures the evolution profiles of most of the intermediate species to a very good level of agreement with significant difference observed in the evolution profile of $CO_2$ only. In addition to the validations shown in Fig. 6 &7, the mechanism was also found to perform well in capturing the evolution of different intermediates during the oxidation of other methylated aromatics as well (c.f., Supplementary material).

### 4.2.4 Laminar flame speed validations

In the final set of validations, the laminar flame speed predictions from the current mechanism were compared against the flame speeds of toluene, *o*-xylene, *p*-xylene, 1,2,4-trimethylbenzene, 1,3,5-trimethylbenzene data of Ji et al. [39] and Dirrenberger et al. [40]. The experiments of [39] suggest that the flame speeds decrease with increasing number of methyl groups on the aromatic ring, while xylene and TMB isomers exhibit identical flame speeds. The mechanism successfully, as seen in Fig. 8, captures these two trends. The decrease in flame speeds with increase in number of methyl groups is

known to be due to the termination reactions of H and benzylic radicals (eg: C6H5CH2+H=toluene) which compete with the high-temperature branching reaction $H+O_2=O+OH$ [16]. The increase in number of methyl groups leads to higher scavenging of H radicals resulting in decrease of the laminar flame speeds. The isomers exhibit similar flame speeds as they exhibit similar reactivity at high temperatures. Finally, regarding the performance of the mechanism in capturing the magnitude of the flame speed, the predicted flame speeds of the xylene and trimethyl benzene isomers match very closely with the reported values of [39], however the peak flame speed of toluene appears to be overpredicted. Figure 8 also shows the comparison of the laminar flame speeds of toluene from the study of Dirrenberger et al. [40] (Open squares in fig.8) which are in closer agreement to the modeling predictions. Comparison of the flame speeds of toluene from studies of Ji et al. [39] and Dirrenberger et al. [40] highlights the possible uncertainty in the flame speeds from literature data and considering this, the performance of the kinetic mechanism is acceptable.

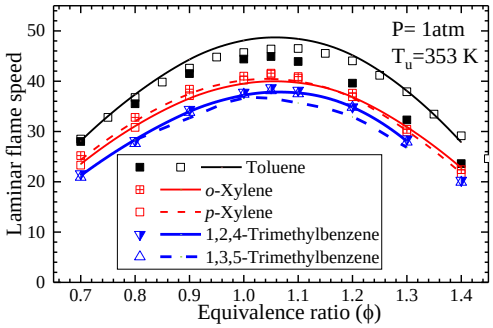


Figure 8: Comparison of experimental and predicted flame speeds of different aromatics [39,40] at atmospheric pressure. For toluene, filled symbols are from [39] and open symbols from [40].

## 5. Conclusion

A detailed kinetic mechanism describing the ignition of toluene, *o*-xylene, *p*-xylene, 1,2,4-trimethylbenzene, 1,3,5-trimethylbenzene and α-methylnaphthalene has been developed. Experiments were also conducted using a rapid compression machine to quantify the ignition response of toluene, *o*-

xylene and 1,2,4-trimethylbenzene at low-to-intermediate temperatures and high pressures. The mechanism has been validated against data sets from both the current experiments and the literature data using ignition delay times, flame speeds and speciation profiles measured in a jet-stirred reactor and flow reactor. Good agreement is observed between the mechanism predictions and the experimental data. The kinetic analysis conducted demonstrates the importance of including the low temperature chemistry of benzylperoxy radicals to accurately capture the ignition propensity of *o*-xylene and 1,2,4-trimethylbenzene at low-to-intermediate temperatures and high pressures. The kinetic mechanism for aromatics developed in the current study could be used for surrogate modeling of a wide range of transportation fuels covering gasoline, jet and diesel fuels.

## 6. Acknowledgements

The work at LLNL was performed under the auspices of the U.S. Department of Energy (DOE), Contract DE-AC52-07NA27344 and was conducted as part of the Co-Optimization of Fuels & Engines (Co-Optima) project sponsored by the DOE Office of Energy Efficiency and Renewable Energy (EERE), Bioenergy Technologies and Vehicle Technologies Offices. The work at ANL is performed under Contract DE-AC02-06CH11357.

## 7. References:

[1] W.J. Pitz, N.P. Cernansky, F.L. Dryer, F.N. Egolfopoulos, J.T. Farrell, D.G. Friend, H. Pitsch, SAE 2007 Transactions Journal of Passenger Cars – Mechanical Systems SAE 2007-01-0175.

[2] J.T. Farrell, N.P. Cernansky, F.L. Dryer, D.G. Friend, C.A. Hergart, C.K. Law, R.M. Mc David, C.J. Mueller, A. K. Patel, H. Pitsch, SAE International 2007-01-0201.

[3] A. Roubaud, R. Minetti, L. R. Sochet, Combust. Flame 121(2000) 535-541.

[4] H. P. S. Shen, J. Vanderover, M.A. Oehlschlaeger, Proc. Combust. Inst. 32 (2009) 165-172.

[5] H. P. S. Shen, M. A. Oehlschlaeger, Combust. Flame 156 (2009) 1053-1062.

[6] P. Dievart, H. H. Kim, S. H. Won, Y. Ju, F.L. Dryer, S. Dooley, W.Wang, , M. A. Oehlschaleger, Fuel 109 (2013) 125-136.

[7] H. Wang, S.J. Warner, M.A. Oehlschlaeger, R. Bounaceur, J. Biet, P.A. Glaude, F. Battin-Leclerc, Combust. Flame 157 (2010), 1976-1988.

[8] W.K. Metcalfe, S. Dooley, F. L. Dryer, Energy and Fuels 25 (2011) 4915-4936.

[9] J. L. Emdee, K. Brezinsky, I. Glassman, Proc. Combust. Inst. 23 (1991) 77-84.

[10] C. R. Shaddix, K. Brezinsky, I. Glassman, Proc. Combust. Inst. 24 (1992) 683-690.

[11] P. Dagaut, G. Pengloan, A. Ristori, Phys. Chem. Chem. Phys. 4 (2002) 1846-1854.

[12] S. Gail, P. Dagaut, Combust. Flame 141 (2005) 281-297.

[13] S. Gail, P. Dagaut, G. Black, J. M. Simmie, Combust. Sci. and Tech. 180 (2008) 1748-1771.

[14] B-Y Wang, D. Yu, G-F Pan, Y-X Liu, J-J Weng, Z- Y Tian, Combust. Flame 192 (2018) 507-516.

[15] J.J. Weng, Y.X Liu, B.Y Wang, L.L. Xing, L.D. Zhang, Z.Y.Tian, Proc. Combust. Inst. 36 (2017) 909-917.

[16] M. Mehl, O. Herbinet, P. Dirrenberger, R. Bounaceur, P. A. Glaude, F. Battin-Leclerc, W. J. Pitz, Proc. Combust. Inst. 35 (2015) 341-348.

[17] Y. Zhang, K.P. Somers, M. Mehl, W.J. Pitz, R.F. Cracknell, H.J. Curran, Proc. Combust. Inst. 36 (2017) 413–421.

[18] Y. Li, C.W. Zhou, K.P. Somers, K. Zhang, and H.J. Curran, Proc. Combust. Inst. 36 (2017) 403–411.

[19] M.A. Oehlschlaeger, D.F. Davidson, R.K. Hanson, Combust. Flame 147(3) (2006) 195-208.

[20] T. Seta, M. Nakajima, A. Miyoshi, Journal of Physical Chemistry A 110 (2006), 5081-5090.

[21] M. Altarawneh, Ala'H. Al-Muhtaseb, B. Z. Dlugogorski, Journal of Computational Chemistry, 32 (2011) 1725-1733.

[22] R.R. Baldwin, M. Scott, R.W. Walker, Combust. Flame 21 (1988) 991–1000.

[23] S.H. Li, J-J Guo, R. Lui, F. Wang, X-Y Li, Journal of Physical Chemistry A 120 (2016), 3424-3432.

[24] A. Elwardany, J. Badra, A. Farooq, Combust. Flame 162 (2015) 2348-2353.

[25] G. da Silva, J. W. Bozzelli, Physical Chemistry Chemical physics 14 (2012) 16143-16154.

[26] G. da Silva, J. W. Bozzelli, Proc. Combust. Inst. 32 (2009) 287–294.

[27] G. da Silva, J. W. Bozzelli, Journal of Chemical Theory and Computation 5 (2009) 3185-3194.

[28] G. da Silva, J. W. Bozzelli, Journal of Physical Chemistry A.113 (2009) 6979-6986.

[29] Y. Murakami, T. Oguchi, K. Hashimoto, Journal of Physical Chemistry A. 111 (2007) 13200-13208.

[30] Y. Murakami, T. Oguchi, K. Hashimoto, Journal of Physical Chemistry A. 113 (2009) 10652-10666.

[31] S. Canneaux, F. Louis, M. Ribaucour, A E. Bakali, Jean-Francois Pawels, Journal of physical chemistry A. 113 (12) 2995-3003.

[32] G. da Silva, J.W. Bozzelli, Combust. Flame 157 (2010) 2175-2193.

[33] A. Mastugi and A. Miyoshi, Intl. J. Chem. Kinetics 44 (3) (2012) 206-218.

[34] G. da Silva, C-C Chen, J.W. Bozzelli, Journal of Physical Chemistry A.111 (35) (2007) 8663-8676.

[35] A. Fridlyand, S.S. Goldsborough, M. Al Rashidi, S.M. Sarathy, M. Mehl, W.J. Pitz, Low temperature autoignition study of substituted 5-membered ring naphthenes, Combust. Flame, submitted.

[36] D.F. Davidson, B.M. Gauthier, R.K. Hanson, Proc. Combust. Inst. 30 (2005) 1175-1182.

[37] G. Mittal, C.-J. Sung, Combust. Flame 150 (2007) 355-368.

[38] G. Kukkadapu, C- J Sung, Energy and Fuels 31 (2017) 854-866.

[39] C. Ji, E. Dames, H. Wang, F.N. Egolfopoulos, Combust. Flame 159 (2012) 1070-1081.

[40] P. Dirrenberger, P.A. Glaude, R. Bounaceur, H. Le Gall, A. Pires da Cruz, A. A. Konnov, F. Battin-Leclerc, Fuel 115 (2014) 162-169.

**List of Figures**

Figure 4: Comparisons of IDT's of monoaromatics (a) toluene [25], (b) *o*-xylene [26], (c) *p*-xylene [26], (d) 1,3,5-trimethylbenzene [27] in air. Constant volume adiabatic simulations were conducted to compare against ST data.

Figure 5: Plot showing comparisons of IDT's of α-methylnaphthalene/air mixtures [28,29]. 0-D simulations with volume histories were conducted for comparing the RCM IDT's.

Figure 6: Comparison of major intermediates produced during oxidation of ϕ=0.977 0.15 % toluene/$O_2$/$N_2$ mixtures [30] at pressure of 12.5 atm in a flow reactor. Experimental data shifted by 0.1 sec.

Figure 7: Comparison of major intermediates produced during JSR oxidation of stochiometric 0.10 % *p*-Xylene/$O_2$/$N_2$ mixtures [35] at atmospheric pressure.

Figure 8: Comparison of experimental and predicted flame speeds of different aromatics [37,38] at atmospheric pressure. For toluene, filled symbols are from [37] and open symbols from [38].

**Supplemental Material**

1. Detailed kinetic mechanism
2. Document with supplemental figures and table
3. Species dictionary containing names of the species in the mechanism and the InChI.
4. Spread sheet summarizing the ignition delay data.
5. Volume histories needed to simulate RCM experiments.